BJU Int 2023 doi:10.1111/bju.16095

Original Article

BJUI
BJU International

Mechanism of urosepsis: relationship between intrarenal pressures and pyelovenous backflow

Anne Hong[1,2], Justin du Plessis[3], Cliodhna Browne[1], Gregory Jack[1] and Damien Bolton[1,4]

[1]*Department of Urology, Austin Health, Heidelberg,* [2]*Faculty of Medicine, Dentistry and Health Sciences, The University of Melbourne, Parkville,* [3]*Department of Anatomical Pathology, Austin Health Pathology, Austin Health, Heidelberg, and* [4]*Department of Surgery, The University of Melbourne, Parkville, Victoria, Australia*

Objective

To document the histological changes observed in renal units subjected to elevated intrarenal pressures (IRPs) and postulate the possible mechanisms of infectious complications after ureteroscopy.

Materials and Methods

Ex vivo studies were performed on porcine renal models. Each ureter was cannulated with a 10-F dual-lumen ureteric catheter. A pressure-sensing wire was inserted through one lumen and with the sensor positioned in the renal pelvis for IRP measurement. Undiluted India ink stain was irrigated through the second lumen. Each renal unit was subjected to ink irrigation at target IRPs of 5 (control), 30, 60, 90, 120, 150, and 200 mmHg. Three renal units were subjected to each target IRP. After irrigation, each renal unit was processed by a uropathologist. Macroscopically, the amount of renal cortex stained by ink was calculated as a percentage of the total perimeter. Microscopically, presence of ink reflux into collecting ducts or distal convoluted tubules, and pressure-related features, was noted at each IRP.

Results

Signs of pressure, as represented by collecting duct dilatation, was first observed at 60 mmHg. Ink staining was consistently observed in the distal convoluted tubules at IRPs ≥60 mmHg, and all renal units above this pressure showed renal cortex involvement. At ≥90 mmHg, ink staining was observed in venous structures. At 200 mmHg, ink staining was observed in supportive tissue, venous tributaries in the sinus fat, peritubular capillaries, and glomerular capillaries.

Conclusion

Using an ex vivo porcine model, pyelovenous backflow occurred at IRPs of ≥90 mmHg. Pyelotubular backflow occurred when irrigation IRPs were ≥60 mmHg. These findings have implications for the development of complications after flexible intrarenal surgery.

Keywords

intrarenal pressure, renal pelvic pressure, pyelovenous backflow, calyceal rupture, ureteroscopy

Introduction

Urolithiasis is a major health problem worldwide and current trends demonstrate increasing prevalence [1,2]. Since the introduction of the flexible ureteroscope [3], flexible intrarenal surgery (FIRS) has become an effective treatment option for both proximal ureteric stones [4,5] and intrarenal stones [6]. However, FIRS is known to lead to raised intrarenal pressures (IRPs) [7], with several studies suggesting that raised IRPs may contribute to higher infectious complications [8]. Various techniques have been suggested to reduce IRPs, such as use of ureteric access sheaths [9], smaller sized ureteroscopes [10], and manipulation of irrigation including isoproterenol irrigation [11]. Given that trends show infectious complications are also increasing over time [12,13], and sepsis being the most common cause of mortality following ureteroscopy for urolithiasis [14], it is pertinent that we understand the mechanism for infections during FIRS to better manage this.

Pyelovenous backflow was described in 1926 by Hinman et al. [15] to be the drainage of fluid into the venous system under raised back pressure from the renal pelvis and has been suggested as a mechanism of pathogenesis for urosepsis. Elevated IRP is recognised during FIRS, and there is evidence to infer a link between this and infectious complications [8,16]. However, backflow of fluid can also occur via several routes, including pyelotubular, pyelosinous, pyelointerstitial,

pyelolymphatic, and pyelovenous [17]; and there is a lack of understanding of how IRPs relate to these forms of backflow. In addition, there are little data to differentiate between fluid backflow and bacterial backflow.

We hypothesise that IRP may affect the kidney in a stepwise manner, starting from the collecting duct of the nephron, then distal tubule, proximal tubule, and later vascular involvement. We aimed to qualify histological changes at specific IRPs, and we postulate the mechanisms that allow ascending urosepsis to develop in patients undergoing FIRS.

Materials and Methods

A total of 21 fresh porcine renal units from female Landrace cross Large White pigs were utilised. Renal units were subjected to targeted IRPs, and each target IRP experiment was performed on three renal units. Significant histological findings for each IRP were assessed on the consistent appearance of a minimum of two out of three renal units.

Intrarenal Pressure Monitoring

The porcine renal units were obtained ex vivo within 30 min of humane sacrifice for the food chain. The setup for IRP monitoring is shown in Fig. 1. Each ureter was cannulated with a 10-F dual-lumen ureteric catheter (Boston Scientific Corporation, Marlborough, MA, USA) with the proximal end at the PUJ. The distal end of the ureter was secured to form a leak-proof seal around the ureteric catheter. A 0.36 mm (0.014″) pressure-sensing wire (Comet II Pressure Guidewire®; Boston Scientific Corporation) was inserted through one lumen and with the sensor positioned in the renal pelvis for IRP measurement. Undiluted India ink stain (Royal Talens, Apeldoorn, the Netherlands) was irrigated manually through the second lumen [18] using a Luer-lock syringe. The IRPs were maintained at the target values by manually adjusting the plunger of the Luer-lock syringe using real-time feedback from the pressure-sensing guidewire. Irrigation was performed for 5 min at the target IRPs of 5 (control), 30, 60, 90, 120, 150, and 200 mmHg.

Macroscopic Examination and Tissue Processing

When irrigation was concluded each kidney was laterally bivalved along the long axis in the coronal plane and fixed in 10% neutral buffered formalin. Fixed organs were photographed, and grossly examined for organ rupture (absent in all cases) and extent of renal parenchymal staining by India ink. Select representative sections were sampled from the most ink-affected areas only, and routine tissue processing was performed (viz., graduated alcohol dehydration, xylene clearing, heated paraffin tissue infiltration, paraffin blocks embedding, 4-µm thick sections cut and stained with haematoxylin and eosin [H&E], mounted to glass slides and coverslipped).

Calculation of macroscopically affected areas in the medulla and cortex were performed to quantify the amount of renal parenchyma macroscopically affected by the ink stain. For the medullary pyramids, each affected pyramid seen on the bivalved view was counted, and the average obtained across three renal units for each target IRP. For cortical involvement, the perimeter of the renal cortex was first measured. The perimeter of the cortex stained by ink was then measured and expressed as a percentage of the total. The mean (±SD) percentage of affected cortex was calculated across the three renal units for each target IRP. The level of ink staining was designated as ‘no staining’, ‘light staining’,

Fig. 1 Experimental setup.

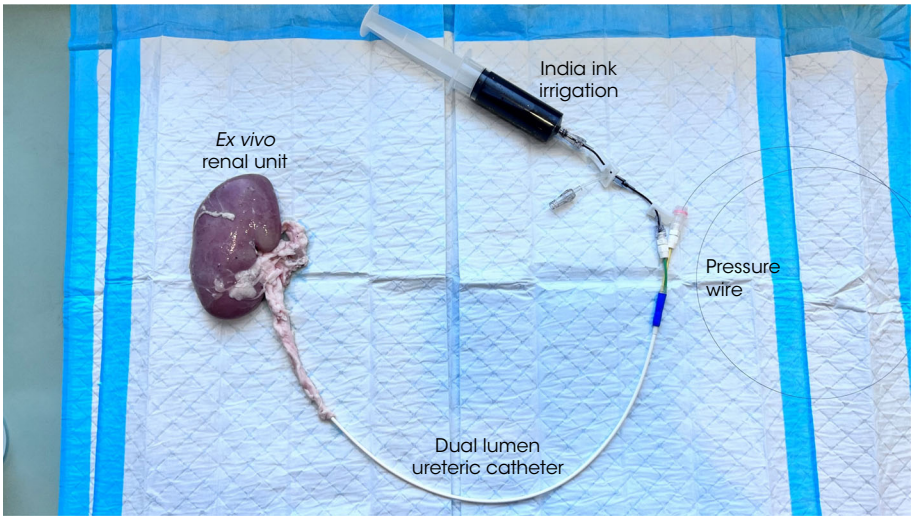

'moderate staining', and 'strong staining' (Fig. S1). The percentage of cortex affected was compared using the Kruskal–Wallis test, with $P \leq 0.05$ representing statistical significance. For purposes of comparison, pressures previously published in referenced articles as centimetres of water (cmH_2O) were converted to mmHg (1 mmHg = 1.3595 cmH_2O).

Histological Assessment

The H&E-stained tissue sections were examined for the presence of India ink reflux into collecting ducts or distal convoluted tubules, and apparent pressure-related features such as collecting duct dilatation, dissection into supportive tissues/interstitium, or ink collecting in parenchymal veins. The findings were reported as either present or absent, with extent of distal convoluted tubule involvement subdivided into <50% or >50%.

Results

Macroscopic Results

The macroscopic results for a representative kidney at each target IRP of 5 (control), 30, 60, 90, 120, 150, and 200 mmHg are shown in Fig. 2. The three control renal units subjected to an IRP of 5 mmHg demonstrated no ink staining of the renal cortex. From 30 mmHg onwards, the renal parenchyma was unevenly affected, with each renal unit containing areas that were macroscopically unstained. The number of renal pyramids and percentage of renal cortex affected is summarised in Table 1. Comparison of renal cortex involvement using the Kruskal–Wallis test did not reveal any significant differences across the targeted IRPs ($P = 0.11$).

Microscopic Results

Three stepwise pathological processes were identified, namely reflux into renal collecting ducts and tubules, ectasia of the collecting ducts, and dissection into stromal tissue. These microscopic results are summarised in Table 2, and examples of each phenomenon are provided in Fig. 3.

Collecting Duct Reflux and Dilatation

Reflux of India ink into the collecting ducts of the renal medulla was the first observed change, starting at pressures as low as 5 mmHg. Pressure-related collecting duct dilatation was first observed at 60 mmHg, with this effect was absent or diminished at ≥150 mmHg.

Fig. 2 Bivalved renal units follow irrigation at intrarenal pressures of (**A**) 5 mmHg, (**B**) 30 mmHg, (**C**) 60 mmHg, (**D**) 90 mmHg, (**E**) 120 mmHg, (**F**) 150 mmHg, and (**G**) 200 mmHg.

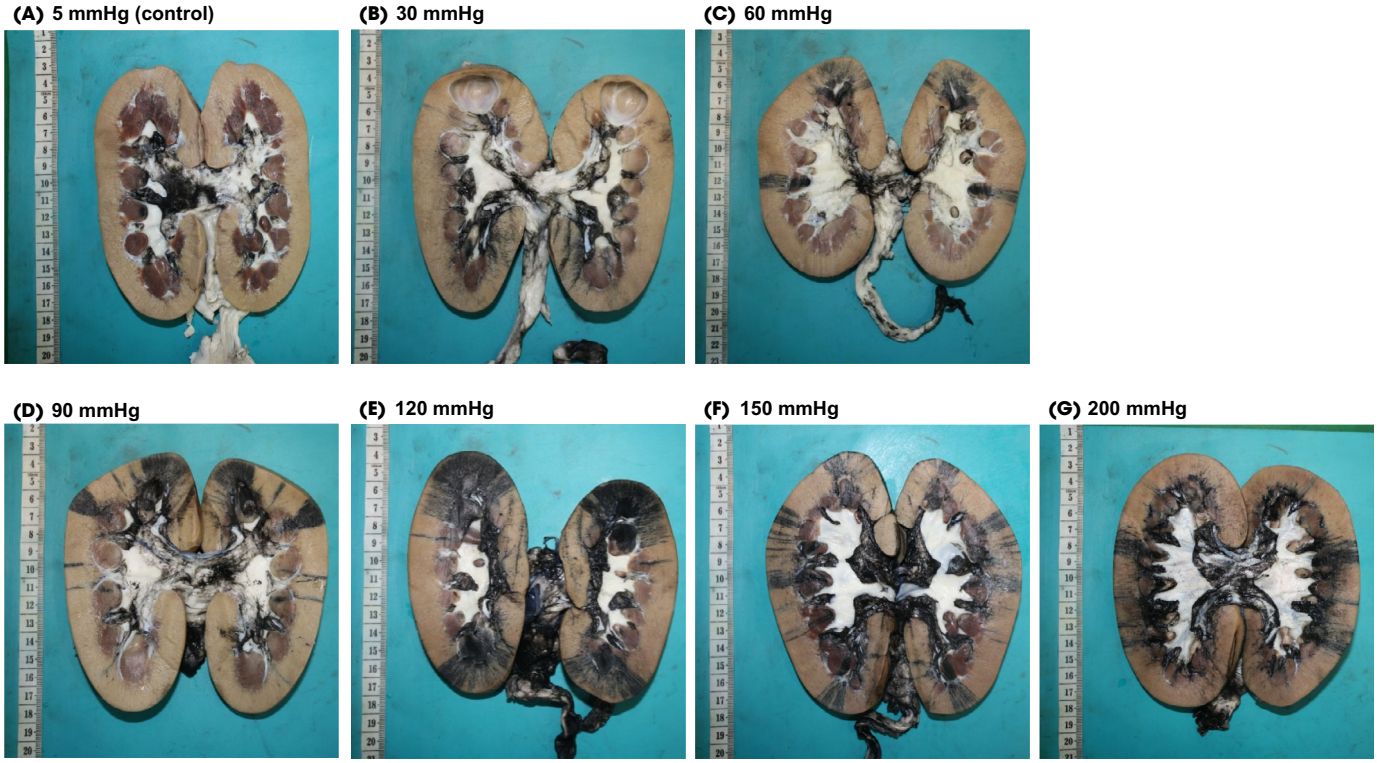

Table 1 Summary of the average macroscopic results for each target IRP (three renal units at each IRP).

IRP, mmHg (3 renal units/group)	Medullary ink staining, *n* stained papillae, mean	Cortex affected by ink stain, %, mean (SD)
5	0	0
30	2.7	18.1 (11.7)
60	3.0	17.8 (4.1)
90	3.3	36.9 (15.3)
120	3.0	37.2 (25.7)
150	3.7	40.1 (23.8)
200	4.6	38.2 (14.0)

Distal Convoluted Tubule Reflux

Backflow of ink into the distal convoluted tubules of the inner cortex first appeared in the renal units subjected to an IRP of 30 mmHg, extending into the outer cortical tubules in all of the renal units subjected to an IRP of 60 mmHg, with this level of involvement present in kidneys at higher pressures.

Venous Involvement

Dissemination of ink into interlobular, arcuate, interlobar, or sinus renal veins was completely absent in all test renal units at an IRP of 5 mmHg, but present in one at 30 mmHg, one at 60 mmHg, two at 90 mmHg, and present in all at 120, 150, and 200 mmHg. At IRPs of 30, 60, 90, and 120 mmHg, reflux was confined to the smaller parenchymal veins (viz. interlobular, arcuate, and interlobar), but at IRPs of 150 and 200 mmHg the larger branches of the renal vein in the sinus were also involved.

Dissection into Supportive Tissues

The ink stain was observed within the supportive tissues of the medulla, cortex or renal sinus in all renal units subjected to an IRP of 200 mmHg, and one unit at 150 mmHg. Minimal microscopic stromal involvement was also seen in one of three renal units at IRPs of 5, 30, and 90 mmHg.

Dissection into Peritubular Interstitium and/or Capillaries

A characteristic delicate lace-like peritubular pattern of ink staining was present in all kidneys at an IRP of 200 mmHg and present in only one renal unit at IRPs of <200 mmHg. The H&E assessment was consistent with localisation both within peritubular capillaries and interstitium.

Involvement of Glomerular Capillaries

This was focally present in two of the renal units subjected to an IRP of 200 mmHg, and very focally present in one 120 mmHg case only. The ink stain was only seen in the glomerular capillaries, and the Bowman's capsules remained ink-stain free in all specimens.

Discussion

In this study macro- and microscopic changes to the renal parenchyma during raised IRPs are described. From these, the contribution of IRPs on the pathogenesis of urosepsis and fluid retention after ureteroscopy may be hypothesised. Stepwise involvement of the structures of the nephron with sequentially higher pressures was observed, from collecting tubules, distal convoluted tubules, venous structures, supportive tissue, and capillaries (Table 2). For ascending urosepsis, bacteria are required to be present in the vascular system and as such pyelotubular backflow and pyelosinus backflow are less likely to contribute to immediate urosepsis than pyelovenous backflow.

Radiological studies as early as 1913 had demonstrated extravasation of contrast material outside of the renal pelvis in conditions of raised IRP [19], but there has been minimal correlation with histological examination. Visualisation of vascular involvement at the microscopic level of the renal unit suggests the contribution of IRP to urosepsis. Limited studies at lower IRPs have previously evaluated this concept, with some evidence of renal parenchymal change on Collargol irrigation and microradiography [19]. In the present study IRPs of ≤60 mmHg demonstrated tubular involvement and those ≥90 mmHg consistently showed venous involvement. It would appear that an IRP of ≥90 mmHg is required to consistently disrupt venous vascular structure in the ex vivo setting.

The exact location of ink stain within the venous system is of interest. At an IRP of 200 mmHg, we found ink staining within large venous tributaries within the renal sinus. IRPs lower than this produced staining only in small venules within the renal parenchyma. This is an important differentiation, as involvement of large veins are more likely to represent immediate bacteraemia, which in turn has implications in higher rates of sepsis and septic shock [20]. With this ink-stain pattern, we hypothesise that an IRP of 200 mmHg may result in a greater likelihood of urosepsis in the immediate postoperative period, while lower IRPs may lead to localised pyelonephritis.

Given that disruption to the tubular epithelium was seen at IRPs as low as 60 mmHg, and the ink stain was seen within the venous system earlier than within the stromal supportive tissue, we postulate that tubular disruption may couple with damage of venous integrity. This barotrauma relieves pressure before the ink reaches the glomerulus, thus the lack of staining observed at the Bowman's capsule.

Fig. 3 Examples of histological findings. (**A**) 5 and 30 mmHg: Section of the medullary papilla with stain seen within the collecting duct but without distension. (**B**) 60 mmHg and 90 mmHg: Section of the medullary papilla with distension of the collecting ducts. (**C**) 120 mmHg: Section of the renal cortex with stain seen within the distal convoluted tubules. (**D**) 120 mmHg: Stain seen within a vein. (**E**) 200 mmHg: Stain seen within an interlobar vein. (**F**) 200 mmHg: Stain seen dissecting into the supportive tissues (here surrounding an interlobar artery). (**G**) 200 mmHg: Stain seen within the peritubular capillaries and interstitium. (**H**) 200 mmHg: Stain seen within the glomerular capillaries but not the Bowman's capsule.

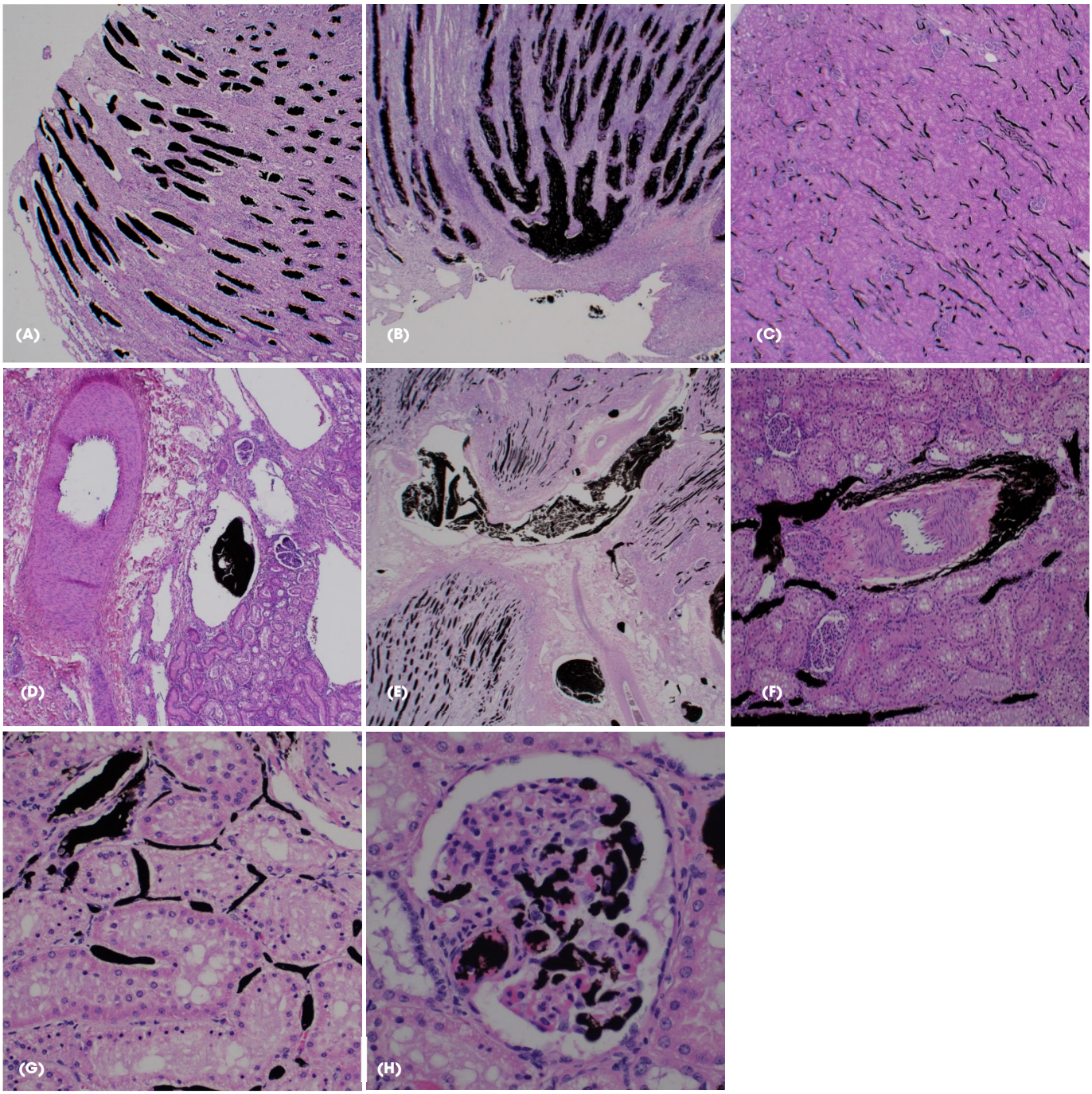

The present study demonstrated some unexpected results. It showed maximal tubular dilatation at 90 and 120 mmHg, but this effect was absent or diminished at ≥150 mmHg. Similar observations were made by Cuttino et al. [21] during microradiography. Coincidentally, at 150 mmHg, there was the first observation of extravasation of ink stain into the supportive tissues of the medulla, cortex, or renal sinus. We hypothesise that forniceal rupture at these pressures leading

Table 2 Summary of microscopic results for all renal units.

IRP, mmHg	Collecting duct involvement	Collecting duct dilatation	Distal convoluted tubule involvement	Venous involvement	Dissection into supportive tissues (medulla, cortex, or renal sinus)	Peritubular capillaries/ Interstitium	Glomerular capillaries
5	+	–	–	–	+	–	–
	+	–	–	–	–	–	–
	–	–	–	–	–	–	–
30	+	–	–	+	+	–	–
	+	–	+	–	–	–	–
	+	–	–	–	–	–	–
60	+	+	+	+	–	–	–
	+	+	+	–	–	–	–
	+	+	+	–	–	–	–
90	+	+	+	+	+	–	–
	+	+	+	–	–	–	–
	+	+	++	+	–	–	–
120	+	+	++	+	–	+	+
	+	+	++	+	–	–	–
	+	+	++	+	–	–	–
150	+	–	+	+	–	–	–
	+	–	+	++	+	–	–
	+	–	++	+	–	–	–
200	+	–	+	++	+	+	+
	+	+	++	++	+	+	–
	+	+	++	++	+	+	+

The "+" designates presence of the feature. For distal convoluted tubule involvement, "+" denotes <50% of cortex involvement and "++" denotes >50% of cortex involvement. For venous involvement "+" represents arcuate or interlobar vein involvement. "++" represents involvement of renal sinus vein tributaries.

to ink stain extravasation relieves the pressure causing collecting system dilatation. Also, each renal unit had areas that were ink-stain free regardless of the target IRP, and no renal units showed equidistant ink stain involvement across the parenchyma. Areas that remain ink-stain free may have been spared as forniceal rupture relieved the pressure effect, and any further pressure effects were preferentially channelled to the rupture (i.e., path of least resistance).

Attention should also be paid to the effects of raised IRPs on the collecting system and tubules, not just the vascular system. The physiological basis of glomerular function is by a pressure differential—the net filtration pressure—thus, the smaller the net filtration, the less fluid is filtered off by the glomerulus. The present study showed that even at an IRP of 5 mmHg, there was ink staining within the collecting tubules. Collecting duct distention was observed at 60 mmHg. Back pressure from the collecting duct at 60 mmHg may infer reduction in the net filtration pressure and may affect renal filtration and fluid retention. Clinically patients with acutely obstructive uropathy (e.g., in the setting of a ureteric stone) have raised IRPs that may exceed 60 mmHg [22] and may experience an acute renal injury, and the above mechanism may be contributing.

A recent study used ethanol irrigation and blood alcohol levels as a marker for pyelovenous backflow in in vivo animal models. It was demonstrated that with higher renal pelvis pressures, there was greater volume of fluids absorbed and at a greater rate [23]. The authors suggest that there may be a pressure threshold above which pyelovenous backflow will occur and that threshold may be somewhere between 55 and 75 mmHg. Our data concurs with this given the pressure effects (i.e., dilatation of collecting ducts) were only evident from 60 mmHg. It should be noted that each ethanol molecule is 0.45 nm in size, with water molecules being 0.28 nm in comparison [24]. As such, the use of ethanol was effective in characterising the pyelovenous migration of small molecules such as water. The present study specifically utilised undiluted India ink as a marker due to the particle size. India Ink particles are 2 μm [25], and the common uropathogens are similar to this (*Escherichia coli*, *Proteus* spp. and *Klebsiella* spp. are ~1 μm [26–28]).

Limitations Exist to this Study

Ex vivo renal units were utilised, and these cannot exactly replicate a living organ. This is a simplified model where only one aspect of pathogenesis of urosepsis is considered. The complexities of immunological and inflammatory responses from the host, endotoxins, blood pressure and muscle tone of the renal pelvis and ureter are not accounted for. Secondly, the renal units are of porcine origin and not human, thus differences exist.

However, porcine models have multipapillate systems, but are also similar in size to that of human kidneys. These features make it the most accurate comparative model available for human renal anatomy. Finally, the renal units were irrigated for 5 min in this study, whereas in vivo flexible ureteroscopies for urolithiasis are performed for a much longer duration [29]. These limitations notwithstanding, the present study is the first to document the histological features of raised IRPs.

Conclusion

Flexible intrarenal surgery is a common treatment method for urolithiasis and septic complications ensue frequently at ~5.0% [16]. The present study demonstrates that pyelotubular and pyelovenous backflow may potentially contribute to the ascending pathway for uropathogens. These results suggest that IRPs of 90 mmHg are required for consistent bacterial pyelovenous backflow. Our results constitute one aspect of IRP and managing complications during ureteroscopy. Human data are limited. Animal models and ex vivo models suggest that IRPs vary greatly during ureteroscopy [7]. Several techniques to reduce IRPs have been examined, including the use of ureteric access sheaths, with increasing size demonstrating better IRP control [30]. Further in vivo studies are required to validate these results.

Author Contributions

Anne Hong: conceptualisation, methodology, formal analysis, investigation, resources, data curation, writing—original draft, writing—review and editing, project administration. **Justin du Plessis:** methodology, data curation, formal analysis, investigation, writing—original draft, writing—review and editing. **Cliodhna Browne:** data analysis, writing—review and editing. **Gregory Jack:** conceptualisation, methodology, writing—review and editing, supervision. **Damien Bolton:** methodology, supervision, writing—review and editing.

Disclosure of Interests

None declared.

Funding

The authors received no financial support for the research, authorship, and/or publication of this article.

References

1 **Abufaraj M, Xu T, Cao C et al.** Prevalence and trends in kidney stone among adults in the USA: analyses of National Health and Nutrition Examination Survey 2007–2018 data. *Eur Urol Focus* 2021; 7: 1468–75

2 **Scales CD Jr, Smith AC, Hanley JM, Saigal CS.** Prevalence of kidney stones in the United States. *Eur Urol* 2012; 62: 160–5

3 **Bagley DH, Huffman JL, Lyon ES.** Flexible ureteropyeloscopy: diagnosis and treatment in the upper urinary tract. *J Urol* 1987; 138: 280–5

4 **Drake T, Grivas N, Dabestani S et al.** What are the benefits and harms of ureteroscopy compared with shock-wave lithotripsy in the treatment of upper ureteral stones? A systematic review. *Eur Urol* 2017; 72: 772–86

5 **Dasgupta R, Cameron S, Aucott L et al.** Shockwave lithotripsy versus ureteroscopic treatment as therapeutic interventions for stones of the ureter (TISU): a multicentre randomised controlled non-inferiority trial. *Eur Urol* 2021; 80: 46–54

6 **Bosio A, Alessandria E, Dalmasso E et al.** Flexible ureterorenoscopy versus shockwave lithotripsy for kidney stones ≤2 cm: a randomized controlled trial. *Eur Urol Focus* 2022; 8: 1816–22

7 **Tokas T, Skolarikos A, Herrmann TRW, Nagele U.** Pressure matters 2: intrarenal pressure ranges during upper-tract endourological procedures. *World J Urol* 2019; 37: 133–42

8 **Farag M, Timm B, Davis N, Wong LM, Bolton DM, Jack GS.** Pressurized-bag irrigation versus hand-operated irrigation pumps during Ureteroscopic laser lithotripsy: comparison of infectious complications. *J Endourol* 2020; 34: 914–8

9 **Auge BK, Pietrow PK, Lallas CD, Raj GV, Santa-Cruz RW, Preminger GM.** Ureteral access sheath provides protection against elevated renal pressures during routine flexible ureteroscopic stone manipulation. *J Endourol* 2004; 18: 33–6

10 **Caballero-Romeu JP, Galán-Llopis JA, Soria F et al.** Micro-ureteroscopy vs. ureteroscopy: effects of miniaturization on renal vascularization and intrapelvic pressure. *World J Urol* 2018; 36: 811–7

11 **Jung H, Nørby B, Frimodt-Møller PC, Osther PJ.** Endoluminal isoproterenol irrigation decreases renal pelvic pressure during flexible ureterorenoscopy: a clinical randomized, controlled study. *Eur Urol* 2008; 54: 1404–13

12 **Whitehurst L, Jones P, Somani BK.** Mortality from kidney stone disease (KSD) as reported in the literature over the last two decades: a systematic review. *World J Urol* 2019; 37: 759–76

13 **Somani BK, Giusti G, Sun Y et al.** Complications associated with ureterorenoscopy (URS) related to treatment of urolithiasis: the Clinical Research Office of Endourological Society URS Global study. *World J Urol* 2017; 35: 675–81

14 **Bhanot R, Pietropaolo A, Tokas T et al.** Predictors and strategies to avoid mortality following ureteroscopy for stone disease: a systematic review from European Association of Urologists Sections of Urolithiasis (EULIS) and Uro-technology (ESUT). *Eur Urol Focus* 2022; 8: 598–607

15 **Hinman F, Redewill FH.** Pyelovenous back flow. *JAMA* 1926; 87: 1287–93

16 **Bhojani N, Miller LE, Bhattacharyya S, Cutone B, Chew BH.** Risk factors for urosepsis after ureteroscopy for stone disease: a systematic review with meta-analysis. *J Endourol* 2021; 35: 991–1000

17 **Harrow BR, Sloane JA.** Pyelorenal extravasation during excretory urography. *J Urol* 1961; 85: 995–1005

18 **Loftus C, Byrne M, Monga M.** High pressure endoscopic irrigation: impact on renal histology. *Int Braz J Urol* 2021; 47: 350–6

19 **Tennant CE.** The cause of pain in pyelography with report of accident and experimental findings. *Ann Surg* 1913; 57: 888–93

20 **Komori A, Abe T, Kushimoto S et al.** Characteristics and outcomes of bacteremia among ICU-admitted patients with severe sepsis. *Sci Rep* 2020; 10: 2983

21 **Cuttino JT Jr, Clark RL, Fried FA, Stevens PS.** Microradiographic demonstration of pyelolymphatic backflow in the porcine kidney. *AJR Am J Roentgenol* 1978; 131: 501–5

22 **Croghan SM, Skolarikos A, Jack GS et al.** Upper urinary tract pressures in endourology: a systematic review of range, variables and implications. *BJU Int* 2022; 131: 267–79

23 **Kottooran C, Twum-Ampofo J, Lee J et al.** Evaluation of fluid absorption during flexible ureteroscopy in an in vivo porcine model. *BJU Int* 2022; 131: 213–8

24 **Li JR, Kuppler RJ, Zhou HC**. Selective gas adsorption and separation in metal-organic frameworks. *Chem Soc Rev* 2009; 38: 1477–504

25 **Royal Talens**. *Royal Talens Ink – Frequently Asked Questions [Webpage]*. Apeldoorn, Netherlands: Royal Talens, 2022. Available at: https://www.royaltalens.com/en/information/frequently-asked-questions/ink/. Accessed September 2022

26 **National Research Council (US) Steering Group for the Workshop on Size Limits of Very Small Microorganisms** ed. *Correlates of Smallest Sizes for Microorganisms. Size Limits of Very Small Microorganisms: Proceedings of a Workshop*. Washington: National Academies Press (US), 1999 ed.

27 **Government of Canada**. Pathogen Safety Data Sheets: Infectious Substances – Proteus spp. Canada 2011. Available at: https://www.canada.ca/en/public-health/services/laboratory-biosafety-biosecurity/pathogen-safety-data-sheets-risk-assessment/proteus.html. Accessed September 2011

28 **Government of Canada**. Pathogen Safety Data Sheets: Infectious Substances – Klebsiella spp. Canada 2011. Available at: https://www.canada.ca/en/public-health/services/laboratory-biosafety-biosecurity/pathogen-safety-data-sheets-risk-assessment/klebsiella.html. Accessed September 2011

29 **Giusti G, Proietti S, Villa L et al.** Current standard technique for modern flexible ureteroscopy: tips and tricks. *Eur Urol* 2016; 70: 188–94

30 **MacCraith E, Yap LC, Elamin M, Patterson K, Brady CM, Hennessey DB**. Evaluation of the impact of ureteroscope, access sheath, and irrigation system selection on intrarenal pressures in a porcine kidney model. *J Endourol* 2020; 35: 512–7

Correspondence: Anne Hong, Department of Urology, Austin Health, 145 Studley Road, Heidelberg, Victoria 3084, Australia.

e-mail: anne.hong@austin.org.au

Abbreviations: FIRS, flexible intrarenal surgery; H&E, haematoxylin and eosin; IRP, intrarenal pressure.

Supporting Information

Additional Supporting Information may be found in the online version of this article:

Fig. S1. Examples of histological findings.

